View metadata, citation and similar papers at core.ac.uk
brought to you by CORE
provided by Elsevier - Publisher Connector

Developmental Cell
Article

Functional Analysis of CTCF During Mammalian Limb Development

Natalia Soshnikova,[1] Thomas Montavon,[2] Marion Leleu,[2] Niels Galjart,[3] and Denis Duboule[1,2,*]
[1]Department of Zoology and Animal Biology, University of Geneva, Sciences III, 1211 Geneva 4, Switzerland
[2]School of Life Sciences, Ecole Polytechnique Fédérale, 1015 Lausanne, Switzerland
[3]Department of Cell Biology and Genetics, Erasmus MC, 3000 DR Rotterdam, the Netherlands
*Correspondence: denis.duboule@epfl.ch or denis.duboule@unige.ch
DOI 10.1016/j.devcel.2010.11.009

SUMMARY

CCCTC-binding factor (CTCF) is a nuclear zinc-finger protein that displays insulating activity in a variety of biological assays. For example, CTCF-binding sites have been suggested to isolate *Hox* gene clusters from neighboring transcriptional interference. We investigated this issue during limb development, where *Hoxd* genes must remain isolated from long-range effects to allow essential regulation within independent sub-groups. We used conditional *Ctcf* inactivation in incipient forelimbs and show that the overall pattern of *Hoxd* gene expression remains unchanged. Transcriptome analysis using tiling arrays covering chromosomes 2 and X confirmed the weak effect of CTCF depletion on global gene regulation. However, *Ctcf* deletion caused massive apoptosis, leading to a nearly complete loss of limb structure at a later stage. We conclude that, at least in this physiological context, rather than being an insulator, CTCF is required for cell survival via the direct transcriptional regulation of target genes critical for cellular homeostasis.

INTRODUCTION

CCCTC-binding factor (CTCF) is a ubiquitous zinc-finger protein with a remarkable structural conservation among many animal species (reviewed in Phillips and Corces, 2009; Ohlsson et al., 2010). CTCF regulates multiple genes and can act either as a repressor, by recruiting the *Sin3a* histone deacetylase and YB-1 transcription factor to target genes (Lutz et al., 2000; Chernukhin et al., 2000), or as an activator by modulating long-range chromatin interactions between enhancers and promoters via intrachromosomal loops (Majumder et al., 2008; Hadjur et al., 2009). These loops may be established either through the formation of CTCF homodimers bound to different genomic loci (Pant et al., 2004; Yusufzai et al., 2004), or via cohesin complexes recruited to DNA in a CTCF-dependent manner (Parelho et al., 2008; Wendt et al., 2008).

The function of CTCF has been investigated in detail during the control of differential gene expression within the *Igf2/H19* imprinted locus (Bell and Felsenfeld, 2000; Hark et al., 2000). At this locus, the same enhancers are required for the activation of both genes, and hence only one gene can be expressed per parental allele (Bartolomei et al., 1993). CTCF prevents de novo DNA methylation of the imprint control region and thus maintains the expression of the maternal *H19* allele (Schoenherr et al., 2003; Fedoriw et al., 2004). Furthermore, it was proposed that CTCF insulates the maternal *Igf2* promoter from the influence of these enhancers by positioning *Igf2* in a transcription inactive chromatin loop (Murrell et al., 2004).

The original suggestion for CTCF displaying an insulating activity derived from an enhancer-blocking assay using a hypersensitive site located upstream the chicken β-*globin* gene in cultured cells. It was proposed that CTCF protects both β-*globin* genes from being silenced by the surrounding heterochromatin, and the neighboring olfactory receptors encoding genes from being activated by the nearby erythroid-specific enhancers (Bell et al., 1999). However, this function was challenged after the deletion of *Ctcf* in erythroid cells did not lead to any ectopic activation of genes adjacent to the β-*globin* locus (Splinter et al., 2006).

Except for few studies where CTCF binding sites were either deleted or mutated (Pant et al., 2004), CTCF function was rarely approached in an organismal context. Analysis of mice carrying a *Ctcf* loss-of-function mutation in $CD4^+$ T cells revealed that this protein regulates cell cycle progression of $\alpha\beta$ T cells in the thymus (Heath et al., 2008). Furthermore, the inactivation or maternal depletion of *Ctcf* in murine oocytes leads to aberrant meiosis and mitosis followed by apoptosis at the four-cell stage (Fedoriw et al., 2004; Wan et al., 2008), illustrating that this factor is essential for the survival of pre-implantation embryos. In humans, mutations in several genes encoding proteins involved in cohesion complex formation, such as *Nipped-B-Like*, *Smc1A*, and *Smc3*, cause the Cornelia de Lange syndrome (CdLS; Dorsett, 2007), whereas mutations in *Esco2*, a gene encoding another regulator of the cohesin complex, are responsible for the Roberts and SC phocomelia syndromes (Dorsett, 2007). Both types of patients display slow growth, mental retardation, and limb defects (Dorsett, 2007). CTCF-dependent changes in the expression of gene important for limb development, in particular of *Hox* genes, were proposed to cause the malformations observed in these patients (Dorsett, 2007; Nasmyth and Haering, 2009).

Hox genes belonging to the *HoxA* and *HoxD* clusters indeed play critical roles during limb development (Zákány and Duboule, 2007). Although the inactivation of both *Hoxd13* and *Hoxa13* results in a lack of digits (Fromental-Ramain et al., 1996),

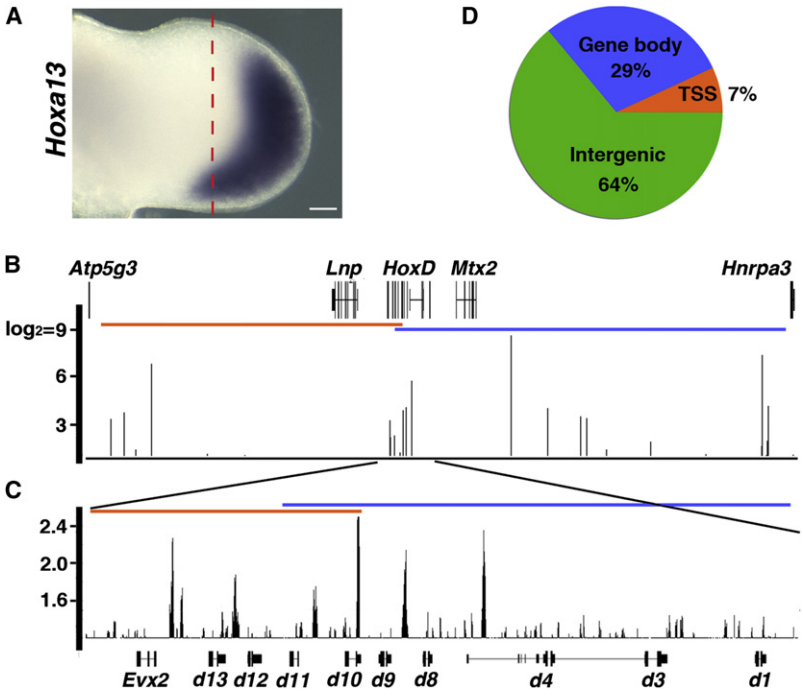

Figure 1. CTCF Binding Sites in Developing Mouse Limbs

(A) A mouse forelimb bud at E10.75, hybridized with a probe specific for *Hoxa13*, which indicates the future autopod domain (hand). The dashed red line indicates the plane of dissection. Scale bar represents 100 μm.

(B) A 2 Mb large region is displayed as an example of CTCF ChIP-chip on a high-density tiling microarrays covering both chromosomes 2, X and Y. CTCF occupancy is shown for the *HoxD* gene cluster as well as for four other genes expressed ubiquitously: *Atp5g3*, *Lnp*, *Mtx2*, and *Hnrpa3*. *Hoxd13* to *Hoxd10* are coexpressed in the developing distal limb (distal to the plane of dissection), along with both *Evx2* and *Lnp*, under the control of enhancers located centromeric (orange line). In parallel, *Hoxd11* to *Hoxd9* are coactivated in the proximal limb domain (proximal to the dissection) by enhancers located telomeric to the cluster (blue line).

(C) A higher magnification of (B) centered on the *HoxD* cluster shows a high density of bound CTCF within this gene cluster, with a clear bias toward the 5′ half of the cluster. The y axis indicates the ratio of ChIP-enriched/input signal intensity, as determined by Bioconductor for (B) or TAS for (C). The position of genes is displayed according to NCBI build 35 of the mouse genome sequence from UCSC genome browser (Kent et al., 2002).

(D) Distribution of CTCF binding sites relative to Refseq genes on chromosomes 2 and X.

Hoxd11 and *Hoxa11* compound mutants have severely truncated zeugopod (forearm, foreleg) elements (Davis et al., 1995) and the combined deletion of both the *HoxA* and *HoxD* clusters almost completely abrogated limb development (Kmita et al., 2005). In developing limb buds, the *Hoxd1* to *Hoxd11* genes first follow a collinear and progressive activation in the presumptive domain of the future forearm (Tarchini and Duboule, 2006). Although the molecular mechanisms responsible for this early phase of activation are as yet poorly understood, this early expression of *Hox* genes contributes to the activation of *Shh* within a small group of posterior mesenchymal cells, the zone of polarizing activity (ZPA; Riddle et al., 1993; Tarchini et al., 2006). SHH, a key molecule for limb outgrowth and patterning (Riddle et al., 1993) is required for the maintenance of *Fgf4* expression in the apical ectodermal ridge (AER; Laufer et al., 1994). Regulatory interactions between SHH and FGF4 are reciprocal, thus leading to a positive feedback loop that promotes limb growth (Laufer et al., 1994; Zuniga et al., 1999).

Along with *Shh* transcriptional activation, a second phase of *Hoxd* genes induction takes place in distal limb bud cells giving rise to the future autopod (Tarchini and Duboule, 2006). This phase involves from *Hoxd10* to *Hoxd13* and is controlled by regulatory sequences located centromeric from the gene cluster (Spitz et al., 2003; 2005; Gonzalez et al., 2007; Montavon et al., 2008). *Lnp* and *Evx2*, two genes located immediately centromeric to the *HoxD* cluster, are coexpressed with *Hoxd* genes in the autopod domain under the control of these potent enhancers. The analyses of spontaneous and genetically engineered mouse mutants have revealed the necessity for a tight regulation of these two partially overlapping groups of *Hoxd* genes, during these early and late phases, to achieve correct limb development. It is particularly critical to isolate the most posterior genes *Hoxd12* and *Hoxd13* from the early regulatory influence, to prevent serious deleterious gain of function effects (Peichel et al., 1997; Herault et al., 1997).

Because genome-wide studies identified CTCF binding sites around and within the *HoxD* cluster in human cells (Kim et al., 2007; Barski et al., 2007), this factor was proposed to function as an insulator to help organizing these regulatory domains (Kim et al., 2007). The mapping of CTCF binding sites to boundary elements at the *AbdominalB Hox* gene locus in *Drosophila* (Holohan et al., 2007) strengthened this assumption. In this study, we report our investigations on the role of CTCF in *Hoxd* genes regulation during limb development, in physiological conditions. We mapped CTCF binding sites in limb mesenchyme for ~10% of the mouse genome. Using a limb conditional mutation of *Ctcf* we identified presumptive target genes, suggesting a function for this protein during limb development. However, neither gene-expression profiling, nor transcriptome analysis indicates that CTCF either directly regulates *Hoxd* genes, or plays a role in insulating groups of genes from undesirable regulations.

RESULTS

Identification of CTCF Binding Sites in Limb Mesenchyme

We mapped CTCF binding sites in mouse limb mesenchyme using chromatin-immunoprecipitation, combined with DNA tiling arrays (ChIP-chip). Chromatin extracts were prepared from the distal part of embryonic limb buds, comprising both the future autopod and zeugopod domains, at day 10.75 of development (E10.75) (Figure 1A). Two biological replicates of ChIP material were hybridized to high density tiling arrays containing nonrepetitive sequences from chromosomes 2, X and Y, i.e., >10% of the mouse genome. The analysis of this data set for chromosomes 2 and X identified 908 enrichment peaks (Figures 1B and 1C), with

peak score ranging from 1.5 to 24.7 (log_2 scale) and an average height and width of 4.3 and 300 bp, respectively. We validated these results by selecting 28 CTCF binding sites with low enrichment scores ($1.5 < x < 2$) and 20 sites with higher enrichment scores ($x > 4.3$) and performed quantitative polymerase chain reaction (PCR) analysis on two independent limb bud samples. Forty-six of forty-eight (95.8%) enrichment peaks were confirmed (see Figure S1 available online).

The analysis of CTCF binding sites distribution relative to annotated genes (Kent et al., 2002) revealed that a large number of sites (64%) locates within intergenic regions (Figure 1D), 29% within genes and 7% near transcription start sites (TSS), defined here as within a one kb window from the TSS. The distribution of peaks within genes and intergenic regions was as expected by a random distribution, in contrast to the recruitments of CTCF to the TSS, which was 5.8-fold higher than expected ($p_{value} < 1 \times 10^{-10}$, χ^2 test). However, binding of CTCF to GC-rich sequences, which are overrepresented within promoters (CpG islands), may explain this bias in peaks' distribution.

We analyzed the *HoxD* cluster in some details by focusing on a 2-mb large DNA interval. This highly syntenic region (Lee et al., 2006a) contains the *HoxD* cluster, the tightly associated *Evx2* gene as well as four ubiquitously expressed genes (*Atp5g3*, *Lnp*, *Mtx2*, *Hnrpa3*) and two gene deserts on either sides with ranges of highly conserved noncoding DNA elements, including enhancer sequences responsible for transcriptional activation of the *Hoxd* genes during limb development (Spitz et al., 2003; Gonzalez et al., 2007) (Figure 1B). We detected four CTCF binding sites ~600 kb upstream the *HoxD* gene cluster and seven sites downstream the cluster (Figure 1B). We considered these as potential candidate sites to either insulate unrelated genes from limb-specific enhancers, or to mediate long-range chromosomal interactions to facilitate selective enhancers-promoters contacts involving specific subset of *Hoxd* genes in each limb domain. Accordingly, we found that seven of nine *Hoxd* genes were flanked by CTCF binding sites (Figure 1C), in particular immediately upstream the TSS of *Evx2*, *Hoxd13*, and *Hoxd12*, supporting a role for CTCF either in the transcriptional activation of these genes during digit development, or alternatively, in their exclusion from the action of forearm enhancers.

CTCF binding sites are generally common to different cell types (Kim et al., 2007; Barski et al., 2007). We compared our data set with that reported for mouse ES cells (Chen et al., 2008), where neither *Hoxd* genes nor *Evx2* are expressed and 14 of our 17 CTCF binding sites were also detected in ES cells (Chen et al., 2008). Furthermore, most of these peaks were also detected in various human cell lines (Kim et al., 2007; Barski et al., 2007). However, the recruitment of CTCF to the promoter of *Evx2* and upstream *Hoxd12* was specific for limb cells (Figure 1C).

Limb Defects in *Ctcf* Conditional Mutant Mice

We assessed the physiological importance of these CTCF binding sites on the regulation of *Hoxd* genes by inactivating *Ctcf* in limb mesenchyme, using a conditional deletion allele (Heath et al., 2008), combined with a *Cre* transgene under the control of the *Prx1* promoter (Logan et al., 2002). After recombination between *loxP* sites flanking the second and the last *Ctcf* exons, a *lacZ* reporter transgene becomes expressed under the control of the endogenous *Ctcf* promoter (Figure 2A),

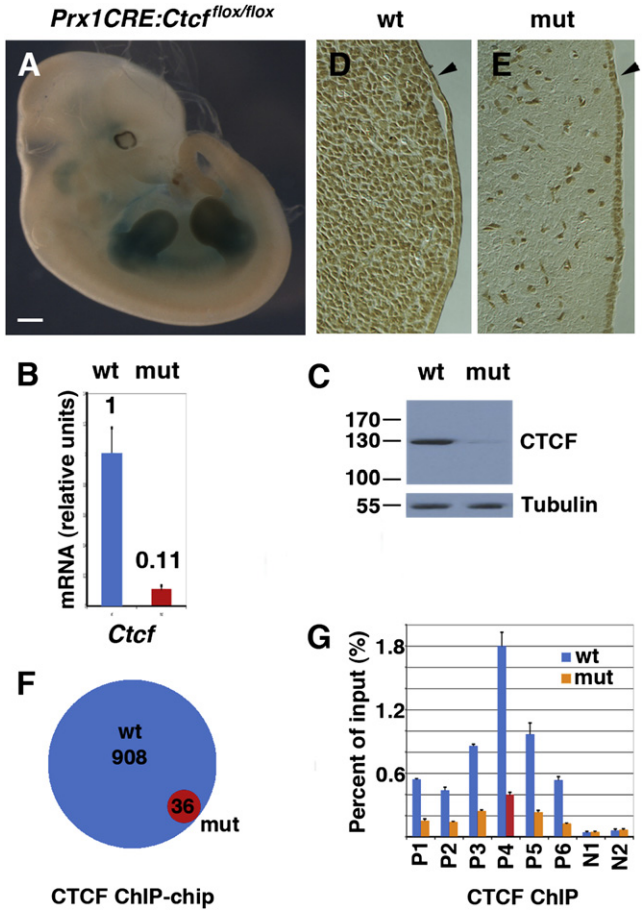

Figure 2. Conditional Inactivation of *Ctcf* in Developing Limbs

(A) β-galactosidase staining in a *Prx1Cre*:*Ctcf*$^{flox/flox}$ embryo, showing the conditional deletion of *Ctcf* in both limb buds at E11.5. After Cre-mediated recombination, *LacZ* becomes expressed under the control of the *Ctcf* promoter. Because the *Prx1Cre* promoter is more efficient in forelimb buds than in hindlimbs, the experiments were all carried out using forelimb bud material. Scale bar represents 600 μm.

(B) Quantitative RT-PCR measuring *Ctcf* transcripts from either wild-type (wt, blue), or *Ctcf* mutant (mut, red) forelimbs at E10.75. Relative *Ctcf* expression level in wild-type was arbitrarily fixed to 1. Error bars are ± SD, n = 3.

(C) Western blot analysis illustrating the almost complete loss of CTCF protein in mutant limbs at E10.75. Tubulin was used as a loading control.

(D) Immuno-histochemical analysis shows the presence of CTCF in both mesenchyme and ectoderm (arrowhead) in wild-type limbs at E10.75. Scale bar represents 20 μm.

(E) CTCF was lost in a vast majority of mesenchymal cells, yet it remained detectable in limb ectoderm (arrowhead) of *Ctcf* mutant embryos, a cell layer where the *Prx1Cre* transgene is not active. Scale bar represents 20 μm.

(F) Venn diagram of CTCF binding events identified by ChIP-chip in wild-type (blue) and *Ctcf* mutant (red) forelimb buds.

(G) ChIP-qPCR analysis for CTCF was performed in wild-type (blue) and *Ctcf* mutant (orange) forelimb buds. CTCF positive (P) and negative (N) sites have the following coordinates: P1 (Chr2:74588380), P2 (Chr2:74610200), P3 (Chr2:74858500), P4 (Chr2:167135300), P5 (Chr2:168268600), P6 (ChrX:154036200), N1 (Chr2:74785900), N2 (Chr2:74807000). Site P4 (red) represents a CTCF binding event identified by ChIP-chip in *Ctcf* mutant forelimb buds. Enrichment is shown as a percentage of input. Error bars are ± SEM, n = 2.

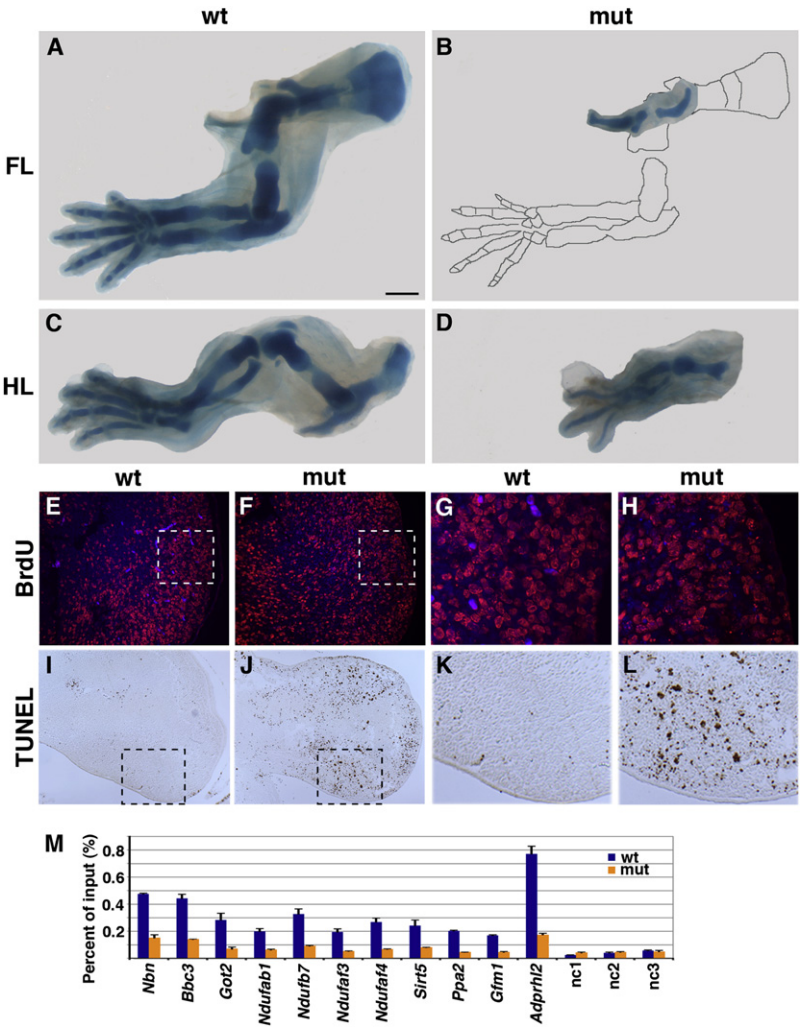

Figure 3. CTCF Is Necessary for Cell Survival During Development

Skeletal preparations of E14.0 wild-type (A and C) and *Prx1Cre*:*Ctcf*$^{flox/flox}$ mutant (B and D) fore- (FL) and hindlimbs (HL). (B) Except for a poorly determined piece of proximal bone, likely part of the clavicle, skeletal elements were absent from *Ctcf* mutant forelimbs. A schematic drawing of wild-type limb skeletal elements is superimposed for comparison. (D) In hindlimbs, a partial deletion of *Ctcf* induced generally ill-formed and shortened limbs, with a reduced number of digits. Scale bars represent 500 μm.

(E–H) BrdU incorporation (red) showing normal proliferation in *Ctcf* mutant limb mesenchyme cells at E11.5. DAPI staining (blue) shows nuclei. (G and H) Enlargements of the areas boxed in (E) and (F). Scale bars represent 75 μm (E and F); 25 μm (G and H).

(I–L) TUNEL assay illustrating the extensive apoptosis in mesenchyme of *Ctcf* mutant forelimbs at E11.5. (K) and (L) are enlargements of the boxed areas in (I) and (J); see also Figure S2. Scale bars represent 150 μm (I and J); 50 μm (K and L).

(M) CTCF ChIP-qPCR analysis for selected target genes identified by expression arrays in wild-type (blue) and *Ctcf* mutant (orange) limb mesenchyme. Enrichment is shown as a percentage of input. Error bars are ± SEM, n = 2.

allowing for the visualization of mutant cells in the limbs. Using quantitative RT-PCR we determined that at least 90% of *Ctcf* RNA was depleted in mutant limbs, as compared to wild-type at E10.75 (Figure 2B). Western blot confirmed the severe reduction of CTCF protein levels in mutant limbs at the same developmental stage (Figure 2C). Furthermore, immunohistochemical analysis showed that CTCF was present in all cells in wild-type limbs (Figure 2D), whereas a vast majority of mesenchymal cells were CTCF negative in mutant limbs (Figure 2E). CTCF protein was expectedly scored in limb ectoderm (Figure 2E), where the *Prx1Cre* transgene is inactive. Importantly, mutant and wild-type limbs were morphologically similar at this developmental stage.

To further quantify the amount of CTCF left in our mutant samples, we carried out an additional ChIP-chip experiment, using *Ctcf* mutant limbs. This data set revealed that 96% of CTCF binding events were lost in the mutant forelimbs at E10.75 (Figures 2F and 2G). Analysis of the remaining 4% indicated that these peaks may represent false positives, as they partly overlap with low complexity or simple repeats regions. We thus concluded that the amount of CTCF in our mutant samples, if not totally abolished, is way below the physiological concentration.

This massive decrease of CTCF lead to a dramatic truncation of the forelimbs, with a detectable size reduction as early as from E11.5 onward. Alcian blue staining of E14.0 embryos indicated that mutant forelimbs lacked all skeletal elements, including the scapula, humerus, radius, ulna, and digits (Figures 3A and 3B). Although hindlimbs were less severely affected, due to the postponed and somewhat lower activity of the *Prx1Cre* transgene there (Logan et al., 2002), mutant skeletal elements were still smaller than wild-type (Figures 3C and 3D). To assess whether such a drastic reduction in limb size was due to a deficit in cellular proliferation or, alternatively, to increased apoptosis, we compared cell proliferation and survival rates in mutant and wild-type embryos. BrdU incorporation was comparable in normal and mutant forelimbs at E11.5 (Figures 3E–3H), suggesting that proliferation was not critically affected. In contrast, apoptosis was strongly enhanced in mutant mesenchymal cells, when compared to wild-type at E11.5 (Figures 3I–3L), indicating that cell survival was strongly impaired in CTCF depleted cells. TUNEL positive cells were found on both anterior and posterior sides of the limb, indiscriminately, though with a higher occurrence within areas of active proliferation.

We further analyzed the molecular consequences of such a depletion of CTCF by genome-wide gene expression profiling using RNA extracted from wild-type and mutant distal limb buds at E10.75. We selected this early developmental stage to look for direct effects, rather than secondary consequences of size reduction, because only few apoptotic cells were scored

in both wild-type and mutant distal limbs (Figure S2). Pair-wise comparison analyses revealed 220 downregulated and 177 upregulated genes, as defined by using a >1.5-fold difference between mutant and wild-type limbs (Tables S1 and S2).

As anticipated from the phenotype, multiple genes encoding apoptotic factors, mitochondrial proteins and enzymes responsible for the reduction of oxidative stress were misregulated in *Ctcf* mutant limbs (Table S3). Furthermore, genes encoding factors involved in the G2/M transition checkpoint were overrepresented (11.7-fold) among deregulated genes, including *Nibrin* (*Nbn*). Yet the largest group of misregulated genes (44 of 397) was concerned with mitochondrial proteins. Although genes encoding subunits of the mitochondrial membrane respiratory chain NADH dehydrogenase complexes (*Ndufab1*, *Ndufb7*, *Ndufaf3*, and *Ndufaf4*), PAR glycohydrolase (*Adprlh2*), Frataxin (*Fxn*), glutamate oxaloacetate transaminase 2 (*Got2*), inorganic pyrophosphatase 2 (*Ppa2*), and Sirtuin 5 deacetylase (*Sirt5*) were downregulated, PUMA (*Bbc3*), which is responsible for the induction of cytochrome c release and apoptosis, was upregulated in *Ctcf* mutant limbs. ChIP-qPCR analyses demonstrated that CTCF was recruited to TSS of all tested downregulated mitochondrial genes and *Bbc3* in mouse limb mesenchyme (Figure 3M).

Effect of CTCF on Transcriptional Regulation

We determined the overall consequences of CTCF depletion on the general transcriptional activity, i.e., including intergenic and intronic noncoding transcripts (ncRNAs), by comparing total RNAs from limb buds of both wild-type and mutant embryos, using tiling arrays covering chromosomes 2, X and Y. Comparative analyses of wild-type and mutant limbs transcript profiles revealed only few differentially expressed genes. Of these, 42 were downregulated, whereas 48 were upregulated by >1.5-fold (Tables S4 and Table S5), which represent ~5% of all genes located on chromosomes 2 and X. The changes in transcripts abundance were arguably moderate, ranging from 1.5- to 2-fold. The results of RNA-chip assay were confirmed on 17 differentially expressed genes by quantitative RT-PCR carried out on three independent limb samples (Figure S3). Fifty-one of fifty-nine (86.5%) genes scored by using the gene expression arrays also appeared as differentially expressed when using RNA-chip on chromosomes 2 and X tiling arrays (Tables S1, S2, S4, and S5).

In contrast, only 65% of those genes identified by RNA-chip were also scored when using the expression arrays. We looked at the correlation between the presence (binding) of CTCF and changes in gene expression. Nineteen genes (45%) detected as being downregulated after CTCF depletion had CTCF recruited to the transcription start site (TSS) in the wild-type condition, whereas nine (22%) had a CTCF binding site within 10 kb from the TSS and 14 (33%) had CTCF binding site further than 10 kb from the TSS (Figure 4A), suggesting that a large fraction of those genes downregulated in *Ctcf* mutant may represent direct targets of CTCF. Likewise, 26% of all genes displaying CTCF bound to their TSS were downregulated in the mutant limbs, indicating that CTCF may exert part of its function by directly activating target promoters.

Among these downregulated genes were *Jag1* and *Grem1* (Figures 4C and 4D), two genes with important functions during limb development (Panman et al., 2006). We detected CTCF recruitment to the TSS of *Jag1* (Figure 4C), as well as to enhancer sequences located within the *Formin* locus (Figure 4D), which are required for the activation of *Grem1* in limb mesenchyme (Zuniga et al., 2004). Moreover, several noncoding RNA genes, such as small nucleolar RNAs, were bound by CTCF and downregulated in *Ctcf* mutant limbs (Figure 4E; Table S1).

We also examined the effect of *Ctcf* loss of function on the transcription of imprinted loci. The transcriptional activity within the *Gnas* cluster (Williamson et al., 2004) was affected in mutant limbs, where we observed a reduced expression of two paternally expressed transcripts, *Nespas* (Nesp antisense) and *Exon 1A*. Accordingly, we identified two CTCF binding sites upstream of the respective promoters (Figure 4F). Changes in gene expression were also detected within the *Dlk1/Gtl2* imprinted locus, as revealed by expression arrays (Table S6). All genes, including paternally expressed *Dlk1* and maternally expressed *Gtl2* and *Rian*, were downregulated >1.5-fold in *Ctcf* mutant limbs. At the *Igf2/H19* locus, we detected a reduced expression of *H19*, yet without any visible gain of *Igf2* expression (Table S6).

In contrast, only two of the upregulated genes (4%) had CTCF bound near their transcription start sites, whereas 11 (23%) displayed CTCF binding within 10 kb from the TSS. Consequently, 35 upregulated genes (73%) were associated with a peak of CTCF occurring >10 kb away from the TSS (Figures 4B and 4G). Genes induced >2-fold belong to this latter category, suggesting that their differential expression is a secondary effect, as supported by their specific expression in muscle (*Dmd* and *Mtmr1*) or ectodermal cells (*Gpc3*, *Gpc4*, *Dlx2*, *Eda2r*). Noteworthy, with the exception of *Eif2s2* and *Phf6*, all upregulated genes were either silent, or expressed at very low levels in wild-type limbs (Figure 4G), making it likely that the observed changes in expression are due to slight modification in the ratio between cells of mesenchymal and nonmesenchymal origin.

Using the chromosomes 2, X and Y tiling arrays, we identified a third class of genes with modified transcriptional activity in *Ctcf* mutant limbs, i.e., those where differential regulation was restricted to intronic sequences (Table S7; Figures 4H and 4I). In all cases, intronic transcripts were downregulated in mutant limbs. Twenty-one of these genes (50%), which were not included in the 42 "downregulated" genes, displayed CTCF binding within the gene body, 13 (29.5%) of which with the binding event within the intron. This group of CTCF targets mostly contained genes encoding multiple isoforms and transcripts lost in the mutant configuration contained either exons used for alternative initiation, cassette exons or retained introns (Kent et al., 2002). However, ~1000 expressed genes located on chromosomes 2 and X did not show splicing defects in mutant limb cells, suggesting that CTCF does not play a generic role in intron excision. Instead, it may regulate the production of specific alternative transcript variants. In summary, CTCF was found to predominantly activate (or derepress) transcription of target genes during limb development. A large number of CTCF-associated genes were not differentially expressed between mutant and wild-type tissues, indicating that the recruitment of CTCF to these sites is not required for proper transcriptional regulation in limb mesenchyme.

Hoxd Genes Expression in *Ctcf* Mutant Limb

Genes located at the 5′ extremity of the *HoxD* cluster, including *Evx2* and from *Hoxd13* until *Hoxd10* were bound by CTCF and

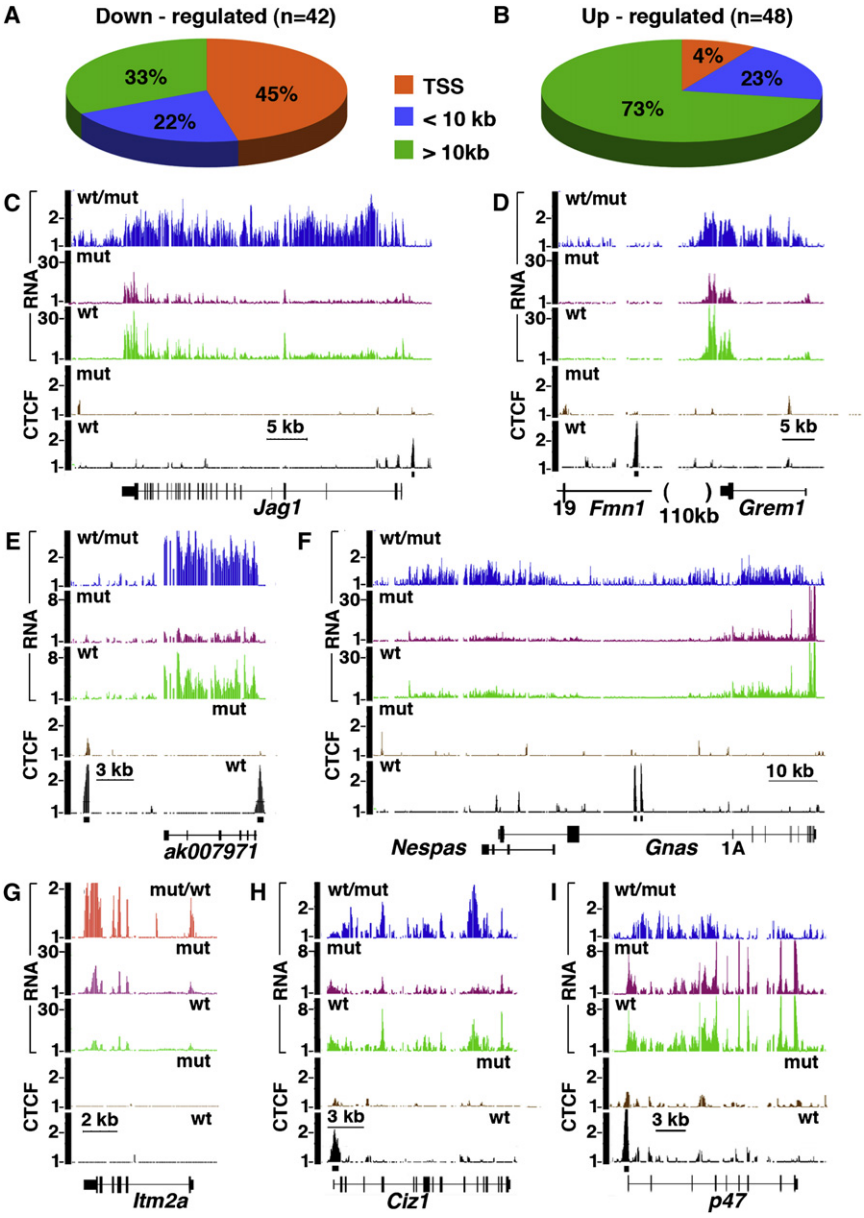

Figure 4. Gene Expression in *Ctcf* Mutant Limbs

(A) Distribution of DNA-bound CTCF relative to the transcription start sites (TSS) of genes downregulated in *Ctcf* mutant limbs at E10.75. CTCF is found either at the TSS (45%), within a 10 kb distance from the TSS (22%) or further away.

(B) Distribution of DNA-bound CTCF relative to the TSS of genes upregulated in *Ctcf* mutant limbs at E10.75.

(C–I) Transcript profiles on high-density tiling microarrays covering both chromosomes 2, X and Y using reverse-transcribed total RNA. The ratio wt/mut signal is shown on the upper profile. Examples are shown for the *Jag1* (C), *Grem1* (D), *ak007971* (E), *Gnas* (F), *Itm2a* (G), *Ciz1* (H), and *p47* (I) genes, in wild-type (green) and *Ctcf* mutant (magenta) limbs. Expression of *Jag1* (C), *Grem1* (D), *ak007971* (E), *Gnas* (F) was downregulated (blue), whereas that of *Itm2a* (G) was increased (red) in *Ctcf* mutant limbs. (H and I) Transcription within introns of the *Ciz1* and *p47* genes was downregulated (blue) in *Ctcf* deficient limbs. CTCF binding sites identified by ChIP-chip are shown for each gene in wild-type (black peaks on the profile at the bottom) or *Ctcf* mutant (brown) limbs. The distance between *Grem1* gene and the CTCF peak located in the intron 19 of *Formin* is of 110 kb (D). The y axis indicates the ratio of cDNA/genomic DNA or ChIP-enriched/input signal intensity.

downregulated in mutant limbs (Figure 5A). In wild-type limb buds, 5′ *Hoxd* genes are transcribed in the autopod (the future hand) with a strict graded quantitative regulation, *Hoxd13* being expressed the strongest whereas *Hoxd9* is barely detectable (Montavon et al., 2008) (Figure 5A). Because *Evx2* is positioned between *Hoxd13* and the autopod specific enhancers, it also falls under the influence of these global enhancers and is thus concomitantly expressed in wild-type autopod (Spitz et al., 2003; Gonzalez et al., 2007; Montavon et al., 2008; Figure 5A).

In *Ctcf* mutant limbs, the transcription of *Evx2* gene was significantly reduced (4.5-fold), whereas *Hoxd13* transcription was moderately changed (2.4-fold reduction) and that of *Hoxd10* virtually unchanged (1.2-fold reduction; Figure 5B). In contrast, RNA levels of the more proximally expressed *Hoxd* genes, such as *Hoxd9* and *Hoxd8* were increased $\leq$3-fold in mutant limbs (Figures 5A and 5B). Whole mount in situ hybridization revealed that *Hoxd13* was expressed in a slightly more restricted area of the posterior-distal part of the developing limb in mutants animals, when compared to wild-type at E10.75 (Figures 5C and 5D). Likewise, *Hoxd10* was detected in almost all cells in wild-type limbs, whereas it appeared downregulated in the anterior part of the *Ctcf* mutant limbs (Figures 5E and 5F). Altogether, the expression patterns of autopod-specific genes, such as *Evx2* and *Hoxd13* were qualitatively similar to wild-type at E11.5 (Figures 5G–5J). *Hoxd10* transcripts were also found at similar levels in both the autopod and posterior zeugopod domains in mutant and wild-type limbs at E11.5 (Figures 5K and 5L). Therefore, during limb development, the activation of *Hoxd* genes by enhancers located on either sides of the gene cluster is largely independent from CTCF.

The ectopic (or elevated) expression of *Hoxd9* was not observed in *Ctcf* mutant limbs, when compared to wild-type at E11.5 or E10.75 (Figures 5M and 5N; Figures S4A and S4B). Furthermore, we did not detect ectopic expression of *Evx2*, *Hoxd13* or of any other *Hoxd* genes analyzed, in either the zeugopod (forearm) or stylopod (arm) domains, indicating that CTCF binding within the *HoxD* cluster is not necessary to insulate posterior *Hoxd* genes from the influence of the early limb enhancers.

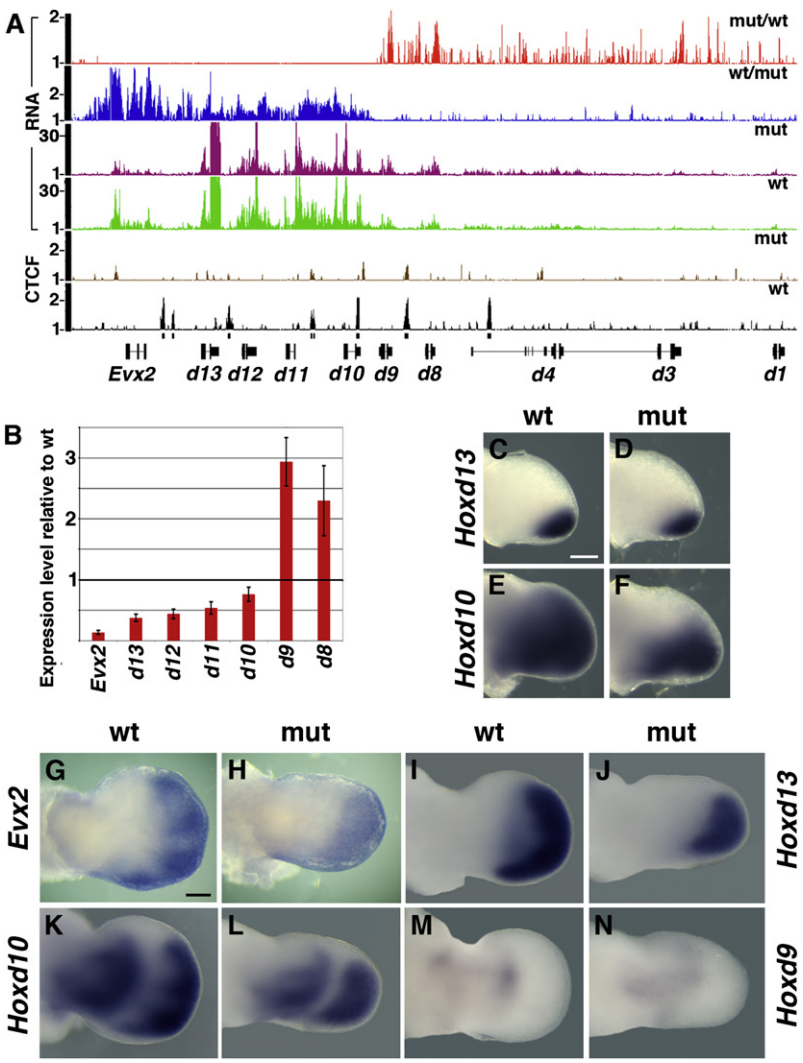

Figure 5. *Hoxd* Genes Expression in Developing *Ctcf* Mutant Limbs

(A) Transcript profiles on high-density tiling microarrays covering chromosomes 2, X and Y using reverse-transcribed total RNA. Transcription of *Hoxd* genes is compared between wild-type (green) and *Ctcf* mutant limbs (magenta). Expression of *Evx2*, *Hoxd13*, to *Hoxd10* genes was reduced in the mutant condition (blue), whereas steady state levels of *Hoxd9* and *Hoxd8* transcripts were slightly increased (red) in *Ctcf* mutant limbs. CTCF binding sites identified by ChIP-chip are shown for each gene in wild-type (black) or *Ctcf* mutant (brown) limbs. The y axis indicates the ratio of cDNA/genomic DNA or ChIP-enriched/input signal intensity.

(B) Quantitative RT-PCR analysis of *Hoxd* genes expression in *Ctcf* mutant limbs at E10.75. Data represent relative expression levels for each gene, as compared to wild-type. Relative expression levels of each gene in wild-type were fixed to 1. Error bars are ± SD, n = 3.

(C–F) Expression patterns of *Hoxd13* (C and D) and *Hoxd10* (E and F) genes in wild-type and mutant forelimb buds at E10.75 (see also Figures S4A and S4B).

(G–N) Expression patterns of *Evx2* (G and H), *Hoxd13* (I and J), *Hoxd10* (K and L), and *Hoxd9* (M and N) genes in wild-type and mutant forelimb buds at E11.5 (see also Figures S4C–S4F). In *Ctcf* deficient limbs, the levels and the spatial distribution of transcripts remained similar to that in wild-type for all genes examined. Noteworthy, the most distal domain (autopod) was reduced in *Ctcf* mutant limbs when compared to wild-type at E11.5. Limb buds are oriented with anterior at the top. Scale bars represent 200 μm.

Loss of *Shh* in *Ctcf* Depleted Limbs

The severe distal truncation of the limb, added to a decrease in the transcription of *5′Hoxd*, *Grem1*, and *Jag1* genes in mutant limbs, suggested that the function of *Sonic hedgehog* (*Shh*) had been affected. Accordingly, we scored a strong downregulation of *Shh* in mutant limbs (Figures 6A and 6B). The expression of *Fgf4*, a gene whose transcription in the apical ectodermal ridge (AER) serves as an indicator of *Shh* activity (Laufer et al., 1994) was also lost (Figures 6C and 6D). In contrast, *Fgf8* expression in the AER was identical between mutant and wild-type limbs (Figures 6E and 6F). *Shh* also regulates the expression of *Grem1* in distal limb mesenchyme (Zuniga et al., 1999), which in turn is required to establish the expression domain of *Jag1* (Panman et al., 2006). Consistently, the expression of both *Grem1* and *Jag1* was strongly decreased in *Ctcf* mutant limbs (Figures 6G–6J).

DISCUSSION

Genome-wide studies have identified >14,000 DNA sites occupied by CTCF in different human and murine cells (Kim et al., 2007; Barski et al., 2007; Chen et al., 2008). However, the biological relevance of this binding was assessed in some details for a few genes only, leading to different suggestions regarding the function of this factor (Schoenherr et al., 2003; Fedoriw et al., 2004; Splinter et al., 2006; Heath et al., 2008; Majumder et al., 2008; Ribeiro de Almeida et al., 2009; Hadjur et al., 2009; Gomes and Espinosa, 2010). We looked at the function of CTCF during early limb development in vivo, using a conditional allele of *Ctcf* in mutant mice, and our mapping of CTCF binding sites identified a majority of DNA fragments located within intergenic regions, far from gene promoters, in agreement with previous studies (Kim et al., 2007; Barski et al., 2007; Chen et al., 2008). Such target sites were proposed to function as insulators, preventing the undesirable activation of genes by tissue specific enhancers located at their vicinity (Kim et al., 2007).

This hypothesis naturally applied to gene members of the *Hoxd* cluster, because a clear partition must exist between expressed and nonexpressed neighboring genes to properly build and pattern our appendages (Zákány and Duboule, 2007). In addition, these complex regulations occur in a genomic region rich in CTCF binding sites and via long-range acting enhancer sequences. However, despite this paradigmatic situation for CTCF acting as an insulator protein, our data do not support this hypothesis and altogether show no evidence for such a function of CTCF, at least in developing limb mesenchyme.

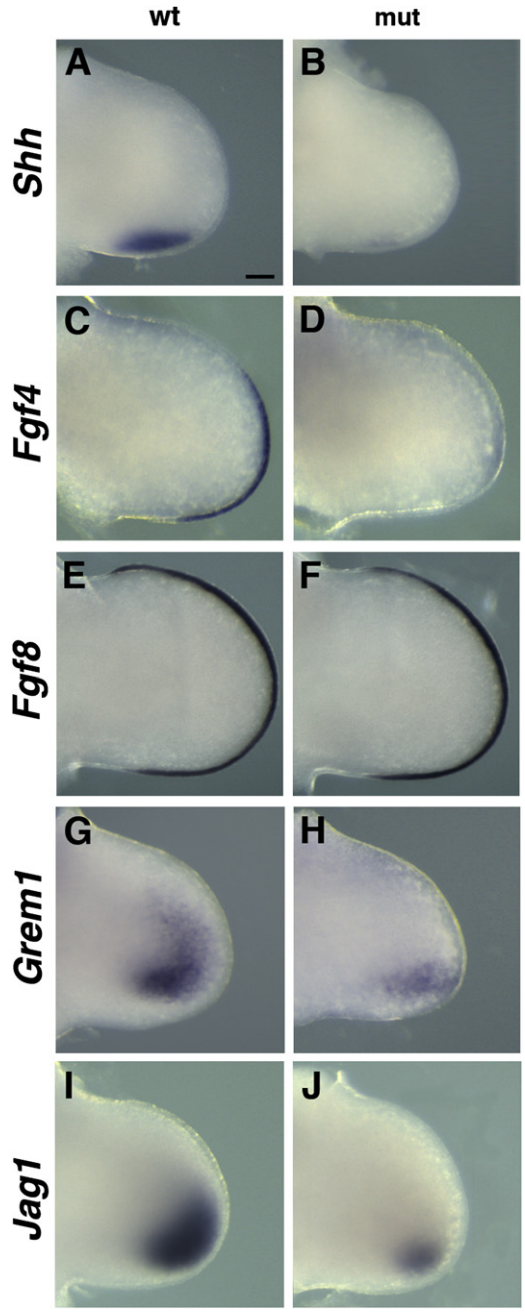

Figure 6. Distal Development in *Ctcf* Mutant Limbs

(A–F) Expression of *Shh* in wild-type (A) and *Ctcf* mutant (B) embryos at E10.5. Expression of *Shh* was strongly downregulated in posterior mutant mesenchyme cells. (C and D) *Fgf4* was lost in the AER of *Ctcf* mutant limbs at E10.75, yet expression of *Fgf8* was as in wild-type embryos at E10.75 (E and F).

(G and H) Expression patterns of *Grem1* in wild-type and *Ctcf* mutant forelimbs at E10.75.

(I and J) *Jag1* expression was downregulated in mutant limb, when compared to wild-type limbs at E10.75. The limb buds are oriented with anterior at the top. Scale bar represents 100 μm.

Expression of *Evx2* and *5′Hoxd* genes, such as *Hoxd13* and *Hoxd12*, was indeed still restricted to the distal part of the limb in *Ctcf* mutant fetuses, much like in wild-type limb buds. This result shows that CTCF is not required for blocking the activation of either *Hoxd13*, or *Hoxd12* in the proximal limb domain (the future forearm) by the early limb enhancers located telomeric to the gene cluster, as suggested by both the presence of CTCF binding sites at the expected locations and the previous observation that these enhancers are capable to ectopically induce the expression of these two genes under experimental conditions (Zákány et al., 2004; Tarchini and Duboule, 2006).

Likewise, *Hoxd* genes expressed in the future forearm region, such as *Hoxd8* or *Hoxd9*, were not dramatically upregulated in most distal cells, after depletion of CTCF, and remained mostly silent in this domain. Therefore, the strict topographic dichotomy in *Hoxd* gene regulation, necessary for proper limb development, was not affected in *Ctcf* mutant appendages. The remaining low amount of CTCF can hardly account for this result. First, only 10% of cells with the floxed *Ctcf* allele still contained enough CTCF to be detected by immunohistochemistry and, consequently, any potential gain of function occurring in CTCF-negative cells should have been scored in our assay. Second, >10% of peaks remained in our mutant samples, when analyzed for CTCF binding events by ChIP.

Multiple CTCF binding sites were also detected at the three paralogous loci, i.e., within the *HoxA*, *HoxB*, and *HoxC* gene clusters (Kim et al., 2007; Barski et al., 2007; Chen et al., 2008), as well as within the *AbdominalB* (*AbdB*) gene locus in *Drosophila* (Holohan et al., 2007), which is the gene cognate of posterior (*Hoxd13* to *Hoxd9*) *Hox* genes in mammals. Yet again, the expression patterns of both *Hoxa13* and *Hoxa11* remained mostly unchanged in *Ctcf* mutant limbs, when compared to wild-type (Figures S4C–S4F). Likewise, we did not detect any ectopic induction of either *Hoxb* or *Hoxc* genes in *Ctcf* mutant limb mesenchyme. This is similar to the case of *Drosophila* CTCF, which binds *Fab-8*, an insulator element required for the restricted expression of *AbdB* in the most posterior segments of *Drosophila* embryo (Moon et al., 2005; Holohan et al., 2007). However, *AbdB* is not expressed ectopically in embryos lacking CTCF. Instead, CTCF is required for the maintenance of *AbdB* expression in its normal domain (Mohan et al., 2007).

Furthermore, mutant limb cells did not overexpress any gene located nearby strongly expressed loci known or suspected to be under the control of remote limb enhancers, including *Shh* (Lettice et al., 2003), *Grem1* (Zuniga et al., 2004), *Bmp2* (Dathe et al., 2009), *Gli3* (Abbasi et al., 2010), or the *HoxA* genes (Lehoczky and Innis, 2008), supporting the conclusion that the precise partition between expressed and nonexpressed genes, often interspersed within one another at these various genomic loci, does not depend (at least solely) on the presence of the CTCF protein. The same conclusion was reached after looking at some loci on chromosomes 2 and X, where no ectopic expression was detected for genes flanking transcriptionally active loci and separated from them by a CTCF binding site(s). For instance, olfactory gene clusters remained transcriptionally silent in *Ctcf* mutant limbs, even though they flank genes highly expressed in limb cells.

Altogether, expression analyses of genes playing key roles during limb morphogenesis did not reveal any obvious

developmental cause of the extreme truncation observed in *Ctcf* mutant forelimbs. Whereas *Shh* expression was strongly weakened, likely impacting on both *Fgf4* and the absolute amount of *Hoxd* transcripts, the phenotype of *Shh* full loss-of-function in forelimbs is not as severe and hence this downregulation of *Shh* may only account for part of the effect. We thus conclude that this striking phenotype is caused by massive cell death, resulting from impairment in a basic cellular process(es), rather than by the misregulation of critical "limb patterning" genes, due to the depletion of CTCF.

In contrast, a clear effect was scored on the transcriptional activation and maintenance of those genes with a TSS bound by CTCF. Within this group, the number of downregulated transcription units was 9-fold higher than the upregulations. CTCF associates with RNA Pol II complexes (Chernukhin et al., 2007) and maintains the expression of imprinted genes by protecting their GC-rich promoters from de novo DNA methylation (Schoenherr et al., 2003; Fedoriw et al., 2004). Accordingly, several imprinted genes, expressed either from the maternal or the paternal alleles, were downregulated in *Ctcf* mutant cells. It was also proposed that CTCF blocks the spreading of a silencing chromatin domain from the neighboring genes or intergenic regions into transcriptionally active loci that escape X chromosome inactivation (Filippova et al., 2005). We did not detect any significant loss of expression for genes located on the X chromosome within regions escaping X-inactivation in female *Ctcf* mutant limbs.

The largest group of downregulated genes in *Ctcf* mutants limb was composed of nuclear genes encoding mitochondrial proteins. These genes are transcriptionally coregulated and the analyses of their core promoters revealed the presence of an ATGGCGG motif (Cunningham et al., 2007), a sequence both known to recruit the transcription factor YY1, and part of the CTCF binding site (Kim et al., 2007; Barski et al., 2007). Our data and genome-wide mapping of CTCF binding sites in human resting $CD4^+$ T cells (Barski et al., 2007) show that all nuclear genes encoding mitochondrial proteins, which are downregulated in *Ctcf* deficient limb mesenchyme, have CTCF bound to their TSS. It is thus possible that CTCF controls cellular homeostasis by directly regulating the transcription of various mitochondrial genes.

Multiple lines of evidence suggest that CTCF is essential for cell survival (Fedoriw et al., 2004; Wan et al., 2008). Consistent with Gomes and Espinosa (2010), we show that the pro-apoptotic gene *Bbc3* (*PUMA*) is likely a direct target of CTCF-mediated repression in limb mesenchyme. Gene expression analysis on chromosomes 2 and X revealed only two genes with CTCF bound at their TSS and upregulated in *Ctcf* mutant limbs, supporting the observation that only a few silent genes display CTCF on their TSS. In fact, the proportion, rather than absolute number, of genes with CTCF at their promoters, which were expressed in control limbs and downregulated in the mutant counterparts was comparable to the proportion of silent genes upregulated in the mutant situation, indicating that CTCF can likely function either as a transcriptional activator or repressor, depending on the recruitment of additional factors.

One-third of CTCF binding sites resides within introns (Kim et al., 2007; this study) and we identified genes showing a downregulation of intronic transcripts only, in CTCF depleted cells. It is thus possible that CTCF activates transcription from cryptic promoters within introns, leading to poorly abundant, noncoding transcripts. Alternatively, CTCF might affect the pre-mRNA splicing by controlling the rate of RNA polymerase II elongation or by recruiting chromatin-modifying enzymes (de la Mata et al., 2003; Luco et al., 2010). The presence of various modifications on histone H3 has been recently associated with either the presence or the absence of alternative exons in mRNAs (Luco et al., 2010) and the correlation between CTCF binding and the tri-methylation of H3K4 at the promoters (Wang et al., 2008) suggests that CTCF could facilitate the positioning of this histone mark over alternatively spliced exons.

EXPERIMENTAL PROCEDURES

Mouse Lines and Genotyping

The $Ctcf^{loxP}$ and *Prx1Cre* mouse lines were described previously (Heath et al., 2008; Logan et al., 2002). Conditional deletion of *Ctcf* in the limb mesenchyme was achieved by crossing *Prx1Cre*:$Ctcf^{loxP}$ heterozygous males with $Ctcf^{loxP}$ heterozygous females. Genotyping of embryos was performed by PCR analysis with the following primers: CTCFfwr: 5′-GAACGAACTAGGCTCAAGA GAG-3′; CTCFrev: 5′-GTGGGCTTCCGGAATAGCTTCC-3′; Prx1fwr: 5′-GGT CTGTAAAACGTCAGGCG-3′; Crerev: 5′-GCGATCCCTGAACATGTCCATCA G-3′; lacZfwr: 5′-GTTAACCGTCACGAGCATCA-3′; lacZrev: 5′-TCACACTCG GGTGATTACGA-3′.

ChIP-Chip

Limb buds were dissected from E10.75 mouse embryos, fixed in 1% formaldehyde for 15 min at room temperature, washed three times with cold phosphate buffer solution (PBS) and stored at −80°C. Pools of 16 limb buds were used for each ChIP-chip experiment. ChIP was performed according to (Lee et al., 2006b) using 2 μg of anti-CTCF antibodies (A300-543A, Bethyl Laboratories) and EZview Red Protein G/A Affinity Gel (Sigma). Immunoprecipitated and whole cell extract DNA (input) were treated with RNaseA, proteinase K and purified by two rounds of extraction with phenol/chloroform/isoamyl alcohol. ChIP and input DNA were amplified using ligation-mediated PCR (Lee et al., 2006b). PCR was limited to 15 cycles. ChIP (1.5 μg) and input DNA were fragmented and labeled using GeneChip WT Double-Stranded DNA Terminal Labeling Kit (Affymetrix) and hybridized to the Chromosome 2 and X tiling arrays (Affymetrix). The arrays are based on NCBI build 33 of the mouse genome (mm5) and contained >6.5 million perfect match oligonucleotide probes positioned every 35 bp mapping to the reverse strand Chromosome 2 and X. Two independent ChIP-chip experiments were performed.

Gene Expression Profiling

Limb buds were dissected from E10.75 mouse embryos and stored in RNAlater reagent (QIAGEN), for genotyping. For each replicate, RNA was isolated from pools of six limb buds either of wild-type or homozygous mutants, using RNeasy micro-kit (QIAGEN). cRNA was synthesized according to the manufacturer's instructions (Ambion) and hybridized to the GeneChip Mouse Genome 430 2.0 Arrays (Affymetrix), which interrogates ~39,000 transcripts. Three independent RNA extractions, cDNA synthesis and array hybridizations were performed. The expression arrays data were normalized and scaled to signal intensity of 100 using GCOS 1.2 software (Affymetrix). Expression levels were analyzed using GeneSpring software (Silicon Genetics, Redwood City, CA) and MATLAB 2009 (The MathWorks, Natick, MA). A 77% cutoff in consistency of change (at least seven of nine comparisons were either increased or decreased) was applied. Only genes that satisfied the pair-wise comparison test and displayed ≥1.5-fold change in expression were considered for further analysis. Gene ontology analysis was performed using the database for annotation, visualization and integrated discovery (DAVID) (Huang da et al., 2009).

Transcript Profiling Using Chromosome 2 and X Tiling Arrays

Limb buds were dissected from E10.75 mouse embryos and stored in RNAlater reagent (QIAGEN), for genotyping. For each replicate, RNA was

isolated from pools of 6 limb buds either of wild-type or homozygous mutants using RNeasy micro-kit (QIAGEN). rRNA was depleted using RiboMinus Human/Mouse Transcriptome Isolation Kit (Invitrogen). After cRNA amplification, single or double-stranded cDNA was generated using The GeneChip Whole Transcript Amplified Double-Stranded Target Assay kit (Affymetrix) according to manufacturer's instructions. cDNA was fragmented and labeled using GeneChip WT Double-Stranded DNA Terminal Labeling Kit (Affymetrix) and hybridized to oligonucleotide tiling arrays. The control genomic DNA samples were fragmented with DNase I. Three independent RNA extractions, cDNA synthesis and array hybridizations were performed.

Analysis of Tiling Array Data

Tiling arrays data were quantile normalized within cDNA/genomic DNA or ChIP/input replicate groups using R packages, STARR and Ringo (Zacher et al., 2010; Toedling et al., 2007). The ratio of probe intensity between the experiment and the control groups were computed considering the median values over replicates. The ratios were smoothened by computing the running medians with a half window size set to 150 bp and a minimum of five probes per window. To identify enriched regions a minimum of three consecutive probes with a smoothed ratio exceeding a threshold have been considered. The threshold has been fixed by taking the 99th percentile of the estimated null distribution of the ratios. Only ChIP enriched regions with score $\log_2 \geq 1.5$ and width ≥ 150 bp were considered for further analysis. RNA-chip data were computed at the exon level, by averaging the normalized intensities of all probes falling within the exon. As a complement, array data were quantile normalized within cDNA/genomic DNA or ChIP/input replicate groups and scaled to medial feature intensity of 10 (transcriptome) or 500 (ChIP-chip) using TAS software (Affymetrix). For each genomic position, a data set was generated consisting of all probes mapping within a sliding window of 80 bp (transcriptome) or 250 bp (ChIP-chip). The averaged ratios were plotted along the genomic DNA sequence using Integrated Genome Browser (IGB) software (Affymetrix).

ChIP-Quantitative Real-Time PCR and Quantitative Reverse-Transcription PCR of mRNA Analyses

To obtain material for homozygous mutants, each pair of limb buds was processed separately and pooled after genotyping. For qRT-PCR, around 150 ng of total RNA from wild-type and *Ctcf* mutant limbs was reverse transcribed using random primers (Invitrogen). Expression changes were then normalized to *Rps9*. PCR primers were designed using Primer Express 2.0 software (Applied Biosystems). ChIP, total genomic DNA (input), and cDNA were PCR amplified using SYBR green containing qPCR master mix kit (Eurogentec) with iCycler (Bio-Rad). A mean quantity was calculated from triplicate reactions for each sample. Primers used are listed in Tables S8–S10.

Histological Techniques and In Situ Hybridization

Wild-type and mutant embryos ($n \geq 5$) were age-matched according to their somite numbers, fixed in 4% formaldehyde in PBS, and processed for paraffin wax embedding. Immunohistochemical analyses were performed on 5-μm paraffin sections using 1:500 anti-CTCF antibody (A300-543A Bethyl Laboratories) and Vectastain Elite ABC kit (Vector Laboratories) according to the manufacture's instructions. BrdU was detected using a 1:250 anti-BrdU antibody (Invitrogen), followed by 1:300 Cy5-conjugated goat anti-mouse secondary antibody (Invitrogen). Apoptotic cells were detected using a DeadEnd Colorimetric TUNEL System (Promega) according to manufacture's instructions. β-galactosidase staining of embryos was performed as described (Spitz et al., 2003). Skeletons of E14.0 embryos were prepared and stained with Alcian blue 8GX. Whole-mount in situ hybridization was performed using digoxigenin-labeled (DIG) RNA probes (Roche) as described (Spitz et al., 2003).

Western Blot

Limb buds were dissected from E10.75 mouse embryos and stored in PBS at −80°C for genotyping. Protein lysates was isolated from pools of six limb buds either of wild-type or homozygous mutants. CTCF protein was detected using a rabbit anti-CTCF antibody (A300-543A, Bethyl Laboratories) and mouse anti-tubulin (T5168 Sigma), with HRP-conjugated secondary antibodies (Sigma) and ECL detection reagents (Perkin-Elmer).

ACCESSION NUMBERS

The data discussed in this publication have been deposited in the European Bioinformatics Institute ArrayExpress and are accessible through numbers E-MEXP-2977, E-MEXP-2979, and E-MEXP-2980.

SUPPLEMENTAL INFORMATION

Supplemental Information includes four figures and ten tables, and can be found with this article online at doi:10.1016/j.devcel.2010.11.009.

ACKNOWLEDGMENTS

We thank J.-C. Martinou and T. Halazonetis for advice, P. Descombes, O. Schaad and members of the NCCR genomics platform for their help with tiling and expression arrays, C. Bauer for help with microscopy as well as members of the Duboule laboratories for discussions and reagents. This work was supported by funds from the University of Geneva, the Ecole Polytechnique Fédérale, Lausanne, the Swiss National Research Fund, the National Research Center (NCCR) "Frontiers in Genetics" the EU program "Crescendo" and the ERC grant Systems*Hox*.ch (to D.D.).

Received: August 2, 2010
Revised: October 17, 2010
Accepted: November 15, 2010
Published: December 13, 2010

REFERENCES

Abbasi, A.A., Paparidis, Z., Malik, S., Bangs, F., Schmidt, A., Koch, S., Lopez-Rios, J., and Grzeschik, K.H. (2010). Human intronic enhancers control distinct sub-domains of Gli3 expression during mouse CNS and limb development. BMC Dev. Biol. *10*, 44.

Barski, A., Cuddapah, S., Cui, K., Roh, T.Y., Schones, D.E., Wang, Z., Wei, G., Chepelev, I., and Zhao, K. (2007). High-resolution profiling of histone methylations in the human genome. Cell *129*, 823–837.

Bartolomei, M.S., Webber, A.L., Brunkow, M.E., and Tilghman, S.M. (1993). Epigenetic mechanisms underlying the imprinting of the mouse H19 gene. Genes Dev. *7*, 1663–1673.

Bell, A.C., and Felsenfeld, G. (2000). Methylation of a CTCF-dependent boundary controls imprinted expression of the Igf2 gene. Nature *405*, 482–485.

Bell, A.C., West, A.G., and Felsenfeld, G. (1999). The protein CTCF is required for the enhancer blocking activity of vertebrate insulators. Cell *98*, 387–396.

Chen, X., Xu, H., Yuan, P., Fang, F., Huss, M., Vega, V.B., Wong, E., Orlov, Y.L., Zhang, W., Jiang, J., et al. (2008). Integration of external signaling pathways with the core transcriptional network in embryonic stem cells. Cell *133*, 1106–1117.

Chernukhin, I.V., Shamsuddin, S., Robinson, A.F., Carne, A.F., Paul, A., El-Kady, A.I., Lobanenkov, V.V., and Klenova, E.M. (2000). Physical and functional interaction between two pluripotent proteins, the Y-box DNA/RNA-binding factor, YB-1, and the multivalent zinc finger factor, CTCF. J. Biol. Chem. *275*, 29915–29921.

Chernukhin, I., Shamsuddin, S., Kang, S.Y., Bergström, R., Kwon, Y.W., Yu, W., Whitehead, J., Mukhopadhyay, R., Docquier, F., Farrar, D., et al. (2007). CTCF interacts with and recruits the largest subunit of RNA polymerase II to CTCF target sites genome-wide. Mol. Cell. Biol. *27*, 1631–1648.

Cunningham, J.T., Rodgers, J.T., Arlow, D.H., Vazquez, F., Mootha, V.K., and Puigserver, P. (2007). mTOR controls mitochondrial oxidative function through a YY1-PGC-1alpha transcriptional complex. Nature *450*, 736–740.

Dathe, K., Kjaer, K.W., Brehm, A., Meinecke, P., Nürnberg, P., Neto, J.C., Brunoni, D., Tommerup, N., Ott, C.E., Klopocki, E., et al. (2009). Duplications involving a conserved regulatory element downstream of BMP2 are associated with brachydactyly type A2. Am. J. Hum. Genet. *84*, 483–492.

Davis, A.P., Witte, D.P., Hsieh-Li, H.M., Potter, S.S., and Capecchi, M.R. (1995). Absence of radius and ulna in mice lacking hoxa-11 and hoxd-11. Nature *375*, 791–795.

de la Mata, M., Alonso, C.R., Kadener, S., Fededa, J.P., Blaustein, M., Pelisch, F., Cramer, P., Bentley, D., and Kornblihtt, A.R. (2003). A slow RNA polymerase II affects alternative splicing in vivo. Mol. Cell *12*, 525–532.

Dorsett, D. (2007). Roles of the sister chromatid cohesion apparatus in gene expression, development, and human syndromes. Chromosoma *116*, 1–13.

Fedoriw, A.M., Stein, P., Svoboda, P., Schultz, R.M., and Bartolomei, M.S. (2004). Transgenic RNAi reveals essential function for CTCF in H19 gene imprinting. Science *303*, 238–240.

Filippova, G.N., Cheng, M.K., Moore, J.M., Truong, J.P., Hu, Y.J., Nguyen, D.K., Tsuchiya, K.D., and Disteche, C.M. (2005). Boundaries between chromosomal domains of X inactivation and escape bind CTCF and lack CpG methylation during early development. Dev. Cell *8*, 31–42.

Fromental-Ramain, C., Warot, X., Messadecq, N., LeMeur, M., Dollé, P., and Chambon, P. (1996). Hoxa-13 and Hoxd-13 play a crucial role in the patterning of the limb autopod. Development *122*, 2997–3011.

Gomes, N.P., and Espinosa, J.M. (2010). Gene-specific repression of the p53 target gene PUMA via intragenic CTCF-Cohesin binding. Genes Dev. *24*, 1022–1034.

Gonzalez, F., Duboule, D., and Spitz, F. (2007). Transgenic analysis of Hoxd gene regulation during digit development. Dev. Biol. *306*, 847–859.

Hadjur, S., Williams, L.M., Ryan, N.K., Cobb, B.S., Sexton, T., Fraser, P., Fisher, A.G., and Merkenschlager, M. (2009). Cohesins form chromosomal cis-interactions at the developmentally regulated IFNG locus. Nature *460*, 410–413.

Hark, A.T., Schoenherr, C.J., Katz, D.J., Ingram, R.S., Levorse, J.M., and Tilghman, S.M. (2000). CTCF mediates methylation-sensitive enhancer-blocking activity at the H19/Igf2 locus. Nature *405*, 486–489.

Heath, H., Ribeiro de Almeida, C., Sleutels, F., Dingjan, G., van de Nobelen, S., Jonkers, I., Ling, K.W., Gribnau, J., Renkawitz, R., Grosveld, F., et al. (2008). CTCF regulates cell cycle progression of alphabeta T cells in the thymus. EMBO J. *27*, 2839–2850.

Herault, Y., Fraudeau, N., Zákány, J., and Duboule, D. (1997). Ulnaless (Ul), a regulatory mutation inducing both loss-of-function and gain-of-function of posterior Hoxd genes. Development *124*, 3493–3500.

Holohan, E.E., Kwong, C., Adryan, B., Bartkuhn, M., Herold, M., Renkawitz, R., Russell, S., and White, R. (2007). CTCF genomic binding sites in Drosophila and the organisation of the bithorax complex. PLoS Genet. *3*, e112.

Huang da, W., Sherman, B.T., and Lempicki, R.A. (2009). Systematic and integrative analysis of large gene lists using DAVID Bioinformatics Resources. Nat. Protoc. *4*, 44–57.

Kent, W.J., Sugnet, C.W., Furey, T.S., Roskin, K.M., Pringle, T.H., Zahler, A.M., and Haussler, D. (2002). The human genome browser at UCSC. Genome Res. *12*, 996–1006.

Kim, T.H., Abdullaev, Z.K., Smith, A.D., Ching, K.A., Loukinov, D.I., Green, R.D., Zhang, M.Q., Lobanenkov, V.V., and Ren, B. (2007). Analysis of the vertebrate insulator protein CTCF-binding sites in the human genome. Cell *128*, 1231–1245.

Kmita, M., Tarchini, B., Zàkàny, J., Logan, M., Tabin, C.J., and Duboule, D. (2005). Early developmental arrest of mammalian limbs lacking HoxA/HoxD gene function. Nature *435*, 1113–1116.

Laufer, E., Nelson, C.E., Johnson, R.L., Morgan, B.A., and Tabin, C. (1994). Sonic hedgehog and Fgf-4 act through a signaling cascade and feedback loop to integrate growth and patterning of the developing limb bud. Cell *79*, 993–1003.

Lee, A.P., Koh, E.G., Tay, A., Brenner, S., and Venkatesh, B. (2006a). Highly conserved syntenic blocks at the vertebrate Hox loci and conserved regulatory elements within and outside Hox gene clusters. Proc. Natl. Acad. Sci. USA *103*, 6994–6999.

Lee, T.I., Johnstone, S.E., and Young, R.A. (2006b). Chromatin immunoprecipitation and microarray-based analysis of protein location. Nat. Protoc. *1*, 729–748.

Lehoczky, J.A., and Innis, J.W. (2008). BAC transgenic analysis reveals enhancers sufficient for Hoxa13 and neighborhood gene expression in mouse embryonic distal limbs and genital bud. Evol. Dev. *10*, 421–432.

Lettice, L.A., Heaney, S.J., Purdie, L.A., Li, L., de Beer, P., Oostra, B.A., Goode, D., Elgar, G., Hill, R.E., and de Graaff, E. (2003). A long-range Shh enhancer regulates expression in the developing limb and fin and is associated with preaxial polydactyly. Hum. Mol. Genet. *12*, 1725–1735.

Logan, M., Martin, J.F., Nagy, A., Lobe, C., Olson, E.N., and Tabin, C.J. (2002). Expression of Cre Recombinase in the developing mouse limb bud driven by a Prxl enhancer. Genesis *33*, 77–80.

Luco, R.F., Pan, Q., Tominaga, K., Blencowe, B.J., Pereira-Smith, O.M., and Misteli, T. (2010). Regulation of alternative splicing by histone modifications. Science *327*, 996–1000.

Lutz, M., Burke, L.J., Barreto, G., Goeman, F., Greb, H., Arnold, R., Schultheiss, H., Brehm, A., Kouzarides, T., Lobanenkov, V., et al. (2000). Transcriptional repression by the insulator protein CTCF involves histone deacetylases. Nucleic Acids Res. *28*, 1707–1713.

Majumder, P., Gomez, J.A., Chadwick, B.P., and Boss, J.M. (2008). The insulator factor CTCF controls MHC class II gene expression and is required for the formation of long-distance chromatin interactions. J. Exp. Med. *205*, 785–798.

Mohan, M., Bartkuhn, M., Herold, M., Philippen, A., Heinl, N., Bardenhagen, I., Leers, J., White, R.A., Renkawitz-Pohl, R., Saumweber, H., et al. (2007). The Drosophila insulator proteins CTCF and CP190 link enhancer blocking to body patterning. EMBO J. *26*, 4203–4214.

Montavon, T., Le Garrec, J.F., Kerszberg, M., and Duboule, D. (2008). Modeling Hox gene regulation in digits: reverse collinearity and the molecular origin of thumbness. Genes Dev. *22*, 346–359.

Moon, H., Filippova, G., Loukinov, D., Pugacheva, E., Chen, Q., Smith, S.T., Munhall, A., Grewe, B., Bartkuhn, M., Arnold, R., et al. (2005). CTCF is conserved from Drosophila to humans and confers enhancer blocking of the Fab-8 insulator. EMBO Rep. *6*, 165–170.

Murrell, A., Heeson, S., and Reik, W. (2004). Interaction between differentially methylated regions partitions the imprinted genes Igf2 and H19 into parent-specific chromatin loops. Nat. Genet. *36*, 889–893.

Nasmyth, K., and Haering, C.H. (2009). Cohesin: its roles and mechanisms. Annu. Rev. Genet. *43*, 525–558.

Ohlsson, R., Lobanenkov, V., and Klenova, E. (2010). Does CTCF mediate between nuclear organization and gene expression? Bioessays *32*, 37–50.

Panman, L., Galli, A., Lagarde, N., Michos, O., Soete, G., Zuniga, A., and Zeller, R. (2006). Differential regulation of gene expression in the digit forming area of the mouse limb bud by SHH and gremlin 1/FGF-mediated epithelial-mesenchymal signalling. Development *133*, 3419–3428.

Pant, V., Kurukuti, S., Pugacheva, E., Shamsuddin, S., Mariano, P., Renkawitz, R., Klenova, E., Lobanenkov, V., and Ohlsson, R. (2004). Mutation of a single CTCF target site within the H19 imprinting control region leads to loss of Igf2 imprinting and complex patterns of de novo methylation upon maternal inheritance. Mol. Cell. Biol. *24*, 3497–3504.

Parelho, V., Hadjur, S., Spivakov, M., Leleu, M., Sauer, S., Gregson, H.C., Jarmuz, A., Canzonetta, C., Webster, Z., Nesterova, T., et al. (2008). Cohesins functionally associate with CTCF on mammalian chromosome arms. Cell *132*, 422–433.

Peichel, C.L., Prabhakaran, B., and Vogt, T.F. (1997). The mouse Ulnaless mutation deregulates posterior HoxD gene expression and alters appendicular patterning. Development *124*, 3481–3492.

Phillips, J.E., and Corces, V.G. (2009). CTCF: master weaver of the genome. Cell *137*, 1194–1211.

Ribeiro de Almeida, C., Heath, H., Krpic, S., Dingjan, G.M., van Hamburg, J.P., Bergen, I., van de Nobelen, S., Sleutels, F., Grosveld, F., Galjart, N., et al. (2009). Critical role for the transcription regulator CCCTC-binding factor in the control of Th2 cytokine expression. J. Immunol. *182*, 999–1010.

Riddle, R.D., Johnson, R.L., Laufer, E., and Tabin, C. (1993). Sonic hedgehog mediates the polarizing activity of the ZPA. Cell *75*, 1401–1416.

Schoenherr, C.J., Levorse, J.M., and Tilghman, S.M. (2003). CTCF maintains differential methylation at the Igf2/H19 locus. Nat. Genet. *33*, 66–69.

Spitz, F., Gonzalez, F., and Duboule, D. (2003). A global control region defines a chromosomal regulatory landscape containing the HoxD cluster. Cell *113*, 405–417.

Spitz, F., Herkenne, C., Morris, M.A., and Duboule, D. (2005). Inversion-induced disruption of the Hoxd cluster leads to the partition of regulatory landscapes. Nat. Genet. *37*, 889–893.

Splinter, E., Heath, H., Kooren, J., Palstra, R.J., Klous, P., Grosveld, F., Galjart, N., and de Laat, W. (2006). CTCF mediates long-range chromatin looping and local histone modification in the beta-globin locus. Genes Dev. *20*, 2349–2354.

Tarchini, B., and Duboule, D. (2006). Control of Hoxd genes' collinearity during early limb development. Dev. Cell *10*, 93–103.

Tarchini, B., Duboule, D., and Kmita, M. (2006). Regulatory constraints in the evolution of the tetrapod limb anterior-posterior polarity. Nature *443*, 985–988.

Toedling, J., Sklyar, O., Krueger, T., Fischer, J.J., Sperling, S., and Huber, W. (2007). Ringo—an R/Bioconductor package for analyzing ChIP-chip readouts. BMC Bioinformatics *8*, 221.

Wan, L.B., Pan, H., Hannenhalli, S., Cheng, Y., Ma, J., Fedoriw, A., Lobanenkov, V., Latham, K.E., Schultz, R.M., and Bartolomei, M.S. (2008). Maternal depletion of CTCF reveals multiple functions during oocyte and preimplantation embryo development. Development *135*, 2729–2738.

Wang, Z., Zang, C., Rosenfeld, J.A., Schones, D.E., Barski, A., Cuddapah, S., Cui, K., Roh, T.Y., Peng, W., Zhang, M.Q., et al. (2008). Combinatorial patterns of histone acetylations and methylations in the human genome. Nat. Genet. *40*, 897–903.

Wendt, K.S., Yoshida, K., Itoh, T., Bando, M., Koch, B., Schirghuber, E., Tsutsumi, S., Nagae, G., Ishihara, K., Mishiro, T., et al. (2008). Cohesin mediates transcriptional insulation by CCCTC-binding factor. Nature *451*, 796–801.

Williamson, C.M., Ball, S.T., Nottingham, W.T., Skinner, J.A., Plagge, A., Turner, M.D., Powles, N., Hough, T., Papworth, D., Fraser, W.D., et al. (2004). A cis-acting control region is required exclusively for the tissue-specific imprinting of Gnas. Nat. Genet. *36*, 894–899.

Yusufzai, T.M., Tagami, H., Nakatani, Y., and Felsenfeld, G. (2004). CTCF tethers an insulator to subnuclear sites, suggesting shared insulator mechanisms across species. Mol. Cell *13*, 291–298.

Zacher, B., Kuan, P.F., and Tresch, A. (2010). Starr: Simple Tiling Array Analysis of Affymetrix ChIP –chip data. BMC Bioinformatics *11*, 194.

Zakany, J., and Duboule, D. (2007). The role of Hox genes during vertebrate limb development. Curr. Opin. Genet. Dev. *17*, 359–366.

Zákány, J., Kmita, M., and Duboule, D. (2004). A dual role for Hox genes in limb anterior-posterior asymmetry. Science *304*, 1669–1672.

Zuniga, A., Haramis, A.P., McMahon, A.P., and Zeller, R. (1999). Signal relay by BMP antagonism controls the SHH/FGF4 feedback loop in vertebrate limb buds. Nature *401*, 598–602.

Zuniga, A., Michos, O., Spitz, F., Haramis, A.P., Panman, L., Galli, A., Vintersten, K., Klasen, C., Mansfield, W., Kuc, S., et al. (2004). Mouse limb deformity mutations disrupt a global control region within the large regulatory landscape required for Gremlin expression. Genes Dev. *18*, 1553–1564.